A quantum electrodynamical theory of differential scattering based on a model with two chromophores

I. Differential Rayleigh scattering of circularly polarized light

BY D. L. ANDREWS AND T. THIRUNAMACHANDRAN

Department of Chemistry, University College, London WC1E 6BT, U.K.

Chiral systems can scatter circularly polarized photons at rates dependent on the handedness of the incident radiation. Differential intensities of Raman scattering by optically active organic molecules have been observed recently. The present work deals with the theory of both Rayleigh and Raman differential scattering by using quantum electrodynamics. The calculations of differential intensities are based on a two-chromophore model in which the chromophores, assumed to be achiral in isolation, become optically active due to their dissymmetric arrangement. Results are reported for both 'in-plane' and 'out-of-plane' polarizations of the scattered radiation. They apply to an arbitrary scattering geometry and group separation. The limiting near- and far-zone behaviour is analysed in detail.

In this paper (part I), the basic theory common to Rayleigh and Raman differential scattering is presented and is then applied to the Rayleigh process. The application to the Raman process is given in part II. In the Rayleigh case, the dominant contribution to the differential effect arises from interference of second-order probability amplitudes. This term varies linearly with the inter-chromophore separation in the near-zone, but inversely in the far-zone. Higher-order corrections to the differential intensities involve coupling between the chromophores; the leading correction, involving the interference of the second- and fourth-order amplitudes, has been computed.

1. INTRODUCTION

Circular dichroism and optical rotation are well-known manifestations of optical activity. Circular dichroism is the property of differential absorption of left and right handed circularly polarized light by chiral molecules; optical rotation is the rotation of the plane of polarization of light. The possibility that optically active systems can show other differential effects has been entertained for a long time. For example, attempts were made long ago to observe differential properties of Rayleigh and Raman scattered light (see, for example, Bhagavantam & Venkateswaran 1930; Kastler 1930). Although these proved unsuccessful, the development of laser technology and sensitive photon counting techniques has recently enabled differential Raman scattering to be observed (Barron, Bogaard & Buckingham 1973).

[297]

Chiral systems may be classified into two types according to which electrons take part in absorption or scattering of light. In the first type, of which hexahelicene is typical, the active electrons are delocalized over a chiral nuclear framework; the system is then said to be inherently optically active. In this type the lack of symmetry usually permits transitions to be electric- and magnetic-dipole allowed simultaneously. A theory of differential scattering by molecules of this kind has been given by Barron & Buckingham (1971). In the second type of system, the active electrons are localized within a functional group which is achiral if its bonding to the rest of the system is ignored. These groups have characteristic absorption bands which are more or less independent of the molecular environment. Examples are the carbonyl, ethylenic and phenyl groups. Many optically active molecules owe their activity to the dissymmetric juxtaposition of such chromophores as in the sterically hindered biphenyls.

Although the optical activity of both these types of system can be treated within the same formalism, better insight is gained if they are treated separately. Our present work is concerned with the latter type. It depends on values of transition moments within the functional groups. Accurate wavefunctions for complicated systems are at present not available and *ab initio* calculations of transition moments are not feasible. Even if such wavefunctions were available, lowest-order transition moment calculations would not be good enough for large molecules. However, transition moments for transitions associated with particular chromophores are available experimentally and these can be used in theoretical models based on coupling between chromophores. A group-coupling model of this kind was used by Kirkwood (1937) to study optical rotation. A similar model has been employed by Barron & Buckingham (1974) in a semi-classical study of differential scattering. (See also Stone 1977.) Their theory is applicable to systems with small group separation.

In this two-part series, we develop the two-group model within the framework of quantum electrodynamics. In our theory, the dynamical system comprises the molecule and the radiation field, and the multipolar Hamiltonian is used to describe it. An important feature of this Hamiltonian is that interactions between molecules or chromophores occur through transverse photon coupling. In part I the quantum electrodynamical theory common to Rayleigh and Raman scattering is described. The theory is applied to the differential scattering process and general expressions are found for differential scattered intensities for incident circularly polarized light. In addition to contributions which arise purely from spatial separation of the chromophores, we evaluate the leading contributions for virtual photon coupling of the chromophores. The derivation is carried out for an arbitrary group separation and scattering geometry; some special cases are discussed. The expressions are analysed for their near- and far-zone behaviour, where the separation is small or large respectively compared with the wavelength of incident light. The leading contributions are found to depend linearly and inversely on the group separation in these regions. In part II (Andrews & Thirunamachandran 1978), **the** theory is applied to differential Raman scattering within the Born–Oppenheimer approximation.

Here the initial and final molecular states are different, in contrast to the Rayleigh process where they are the same. This leads to different results for identical and non-identical chromophores.

2. THEORY

In quantum electrodynamics the dynamical system consists of both the molecules and the radiation field and the Hamiltonian for the system is

$$H = H_{\text{mol}} + H_{\text{rad}} + H_{\text{int}}, \tag{1}$$

where H_{mol} is the non-relativistic Schrödinger operator for the molecules and is assumed known. In contrast to semi-classical theories the radiation field is second-quantized; its Hamiltonian is

$$H_{\text{rad}} = (1/8\pi) \int (e^{\perp 2} + b^2) \, \mathrm{d}^3 r, \tag{2}$$

where $e^\perp$ and b are the microscopic transverse electric and magnetic field operators with plane-wave expansions,

$$e^\perp(r) = \sum_{k, \lambda} (2\pi\hbar ck/V)^{\frac{1}{2}} \, \mathrm{i}[e^{(\lambda)}(k) \, a^{(\lambda)}(k) \, \mathrm{e}^{\mathrm{i}k \cdot r} - \bar{e}^{(\lambda)}(k) \, a^{\dagger(\lambda)}(k) \, \mathrm{e}^{-\mathrm{i}k \cdot r}] \tag{3}$$

and

$$b(r) = \sum_{k, \lambda} (2\pi\hbar ck/V)^{\frac{1}{2}} \, \mathrm{i}[(\hat{k} \times e^{(\lambda)}(k)) \, a^{(\lambda)}(k) \, \mathrm{e}^{\mathrm{i}k \cdot r} - (\hat{k} \times \bar{e}^{(\lambda)}(k)) \, a^{\dagger(\lambda)}(k) \, \mathrm{e}^{-\mathrm{i}k \cdot r}]. \tag{4}$$

In equations (3) and (4), $a^{(\lambda)}(k)$ and $a^{\dagger(\lambda)}(k)$ are the annihilation and creation operators for a photon of wave vector k (frequency $\omega = c \, |k|$) and polarization vector $e^{(\lambda)}$; V is the volume of the quantization box. As shown elsewhere (Babiker, Power & Thirunamachandran 1974), the interaction Hamiltonian may be written as

$$H_{\text{int}} = -\int p(r) \cdot e^\perp(r) \, \mathrm{d}^3 r - \int m(r) \cdot b(r) \, \mathrm{d}^3 r + \tfrac{1}{2} \int O(r, r') : b(r) \, b(r') \, \mathrm{d}^3 r \, \mathrm{d}^3 r', \tag{5}$$

where $p(r)$, $m(r)$ and $O(r, r')$ are the electric polarization, magnetization and diamagnetization fields for the molecular assembly.

For the two-group model, it is sufficient to consider the active electrons of the chromophores. Thus, the Hamiltonian for a two-chromophore system interacting with the radiation field may be written as

$$\begin{aligned} H &= H^{\text{A}} + H^{\text{B}} + H_{\text{rad}} + H_{\text{int}}^{\text{A}} + H_{\text{int}}^{\text{B}} \\ &= H_0 + H_{\text{int}}^{\text{A}} + H_{\text{int}}^{\text{B}}, \end{aligned} \tag{6}$$

where H^{A} and H^{B} are the effective Hamiltonian operators for the chromophores A and B. In (6) we have assumed that the two chromophores are sufficiently far apart to allow electron exchange to be neglected.

In many systems of physical interest the chromophores A and B are optically inactive in isolation but are juxtaposed in a dissymmetric configuration to give chiral character to the pair. Since the intense transitions of the chromophores are

electric-dipole allowed, we use the electric-dipole approximation to the interaction Hamiltonian,

$$H_{\text{int}} \approx e \sum_\alpha (q_{\alpha(A)} - R_A) \cdot e^\perp(R_A) + e \sum_\alpha (q_{\alpha(B)} - R_B) \cdot e^\perp(R_B)$$

$$= - {}^A\mu \cdot e^\perp(R_A) - {}^B\mu \cdot e^\perp(R_B), \tag{7}$$

where $q_{\alpha(\xi)}(\xi = A, B)$ is the coordinate of electron $\alpha(\xi)$ associated with chromophore ξ centred at R_ξ. It is important to emphasize that the electric dipole approximation is with respect to the chromophore and not to the pair. The electric dipole approximation may be relaxed, if necessary, and higher multipolar interactions can be included in a straightforward manner.

Let the initial state of the system be $|0^A 0^B;\ ke^{(\text{L/R})}\rangle$, where $|0^A\rangle$, $|0^B\rangle$ are the ground-state vectors of A, B, and $|ke^{(\text{L/R})}\rangle$ is the state vector of the incident photon with left or right handed circular polarization. Since we are concerned with elastic scattering, the final state is $|0^A 0^B;\ k'e'\rangle$, where the scattered photon is represented by $|k'e'\rangle$ with $|k'| = |k|$. The scattering rate for the process is calculated from Fermi golden rule,

$$\Gamma = (2\pi/\hbar) |M|^2 \rho_f, \tag{8}$$

where ρ_f is the density of final states and the matrix element M is

$$M = \langle k'e';\ 0^B 0^A |\hat{M}| 0^A 0^B;\ ke^{(\text{L/R})}\rangle. \tag{9}$$

Since the overall process involves a change of two photons, only even orders in H_{int} contribute to the matrix element. Thus the operator $\hat{M}$ in (9) is given by

$$\hat{M} = H_{\text{int}} \frac{1}{E - H_0} H_{\text{int}} + H_{\text{int}} \frac{1}{E - H_0} H_{\text{int}} \frac{1}{E - H_0} H_{\text{int}} \frac{1}{E - H_0} H_{\text{int}} + \dots. \tag{10}$$

The leading term, of second order, corresponds to scattering by uncoupled individual chromophores. We call this a 'one-centre' process; the various possibilities are represented by time-ordered diagrams in figure 1. Figures 1a and b are for scattering by chromophore A, and figures 1c and d for the scattering at B.

The next contributions to (9) come from fourth-order perturbation and involve coupling between the two groups. They may be conveniently divided into two sets. The first, which we refer to as set $\{\alpha\}$, is the case in which the photons $|ke^{(\text{L/R})}\rangle$ and $|k'e'\rangle$ are incident on and emergent from different chromophores with virtual photon coupling. A total of 48 graphs is required, falling into four subsets of twelve diagrams each. Figure 2a shows a typical member of the first subset, in which the incidence of the real photon and emission of the virtual photon both take place at A. A second subset with the virtual photon propagating from B to A is typified by figure 2b; (c) and (d) show examples of the remaining two subsets which are reflexions of (a) and (b), in the sense that the real photons are absorbed at B and emitted at A. The other fourth-order set $\{\beta\}$, comprising 48 graphs, belongs to the case where the absorption and emission of the real photons occur at the same centre, the two
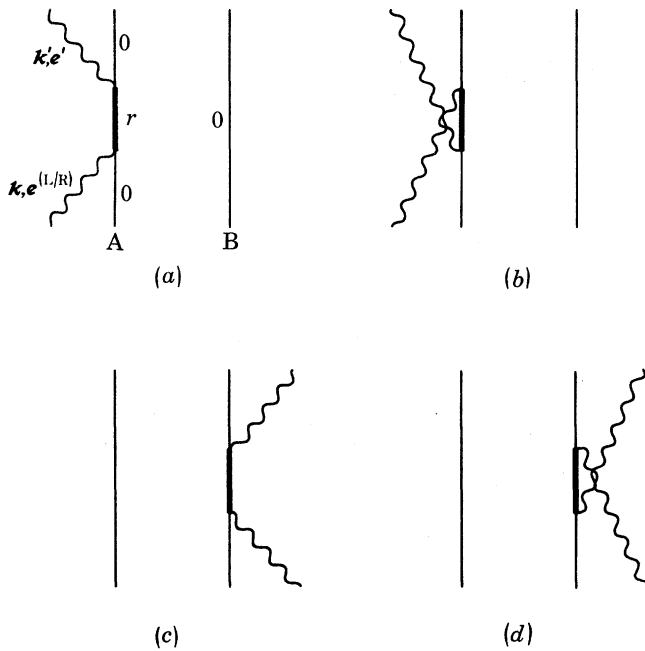
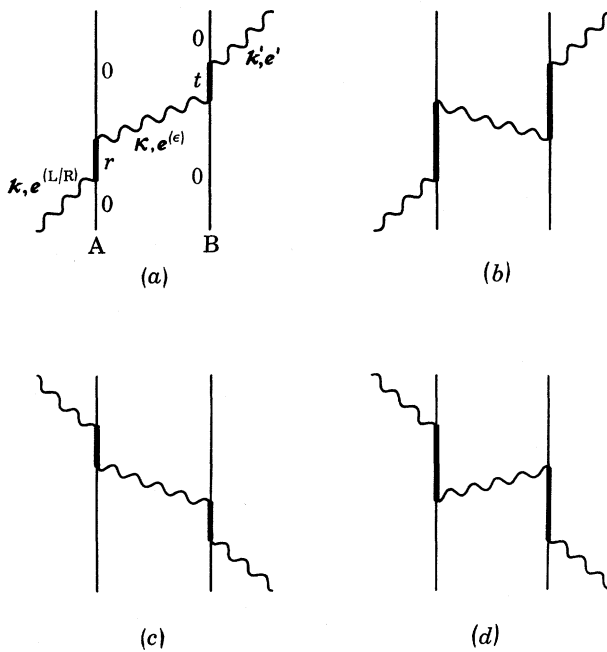FIGURE 1. Time-ordered diagrams for second-order matrix elements.

FIGURE 2. Typical fourth-order diagrams belonging to set $\{\alpha\}$.

centres being coupled by a virtual photon. These graphs also fall into four subsets, typical members of which are shown in figure 3.

Using the interaction Hamiltonian (7) we now calculate the matrix element (9). The second-order contribution to the matrix element is easily computed with the aid of the time-ordered diagrams and is

$$M_2(\text{L/R}) = -(2\pi\hbar ck/V)\,\bar{e}'_i e_j^{(\text{L/R})}[^{\text{A}}\alpha_{ij}(k) + {}^{\text{B}}\alpha_{ij}(k)\,\mathrm{e}^{\mathrm{i}(k-k')\cdot R}]. \qquad (11)$$

In (11) $^{\text{A}}\alpha_{ij}(k)$ is the dynamic polarizability tensor for group A,

$$^{\text{A}}\alpha_{ij}(k) = \sum_r \left\{ \frac{^{\text{A}}\mu_i^{0r}\,{}^{\text{A}}\mu_j^{r0}}{E_{r0}^{\text{A}} - \hbar ck} + \frac{^{\text{A}}\mu_j^{0r}\,{}^{\text{A}}\mu_i^{r0}}{E_{r0}^{\text{A}} + \hbar ck} \right\} \qquad (12)$$

with summation over the intermediate states $|r\rangle$ of A. We have chosen A as the origin; R is the vector $\overrightarrow{\text{AB}}$. The exponential factor in (11) brings in the retardation effects and hence the relative position dependence.
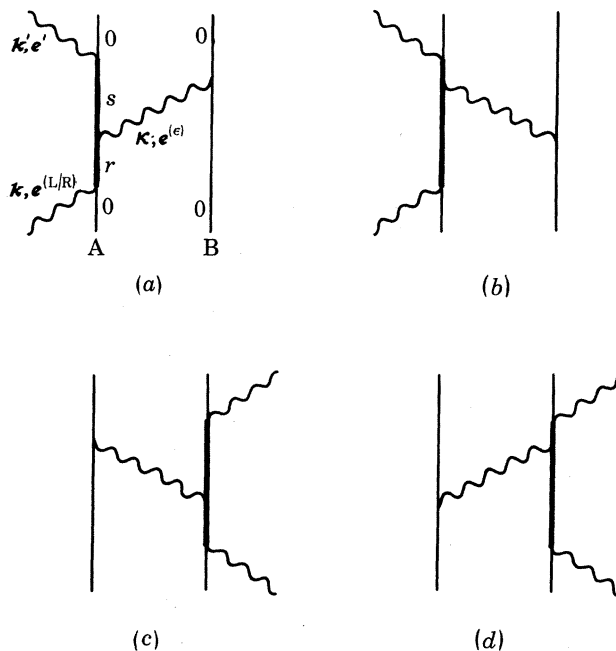
FIGURE 3. Typical fourth-order diagrams belonging to set $\{\beta\}$.

The fourth-order contributions to the matrix element may be considered as a a sum of set $\{\alpha\}$ and set $\{\beta\}$ terms. Proceeding in the conventional manner, we find that the contributions from the twelve graphs of type α in figure 2 may be summed to give

$$\left(\frac{4\pi^2\hbar ck}{V^2}\right)\bar{e}'_i e_j^{(\text{L/R})}\,{}^{\text{B}}\alpha_{im}(k)\,{}^{\text{A}}\alpha_{nj}(k)\,\mathrm{e}^{-\mathrm{i}k'\cdot R}\sum_{\kappa,\,\epsilon}\frac{\hbar c\kappa e_m^{(\epsilon)}(\kappa)\,\bar{e}_n^{(\epsilon)}(\kappa)}{\hbar ck - \hbar c\kappa}\,\mathrm{e}^{\mathrm{i}\kappa\cdot R}. \qquad (13)$$

In (13) $\boldsymbol{\kappa}$ and ϵ are the wave vector and the polarization index of the virtual photon. The matrix elements from the other set $\{\alpha\}$ graphs may be summed in a similar fashion and we obtain for the total contribution from this set

$$
\begin{aligned}
M_{4\alpha}(\mathrm{L/R}) = & \left(\frac{4\pi^2\hbar ck}{V^2}\right) \bar{e}'_i e_j^{(L/R)} \left[{}^{\mathrm{B}}\alpha_{im}(k)\,{}^{\mathrm{A}}\alpha_{nj}(k)\,\mathrm{e}^{-\mathrm{i}\boldsymbol{k}'\cdot\boldsymbol{R}} \right. \\
& \times \sum_{\boldsymbol{\kappa},\,\epsilon} \left\{ e_m^{(\epsilon)}(\boldsymbol{\kappa})\,\bar{e}_n^{(\epsilon)}(\boldsymbol{\kappa}) \frac{\hbar c\kappa}{\hbar ck-\hbar c\kappa}\,\mathrm{e}^{\mathrm{i}\boldsymbol{\kappa}\cdot\boldsymbol{R}} + \bar{e}_m^{(\epsilon)}(\boldsymbol{\kappa})\,e_n^{(\epsilon)}(\boldsymbol{\kappa}) \frac{\hbar c\kappa}{-\hbar ck-\hbar c\kappa}\,\mathrm{e}^{-\mathrm{i}\boldsymbol{\kappa}\cdot\boldsymbol{R}} \right\} \\
& + {}^{\mathrm{B}}\alpha_{nj}(k)\,{}^{\mathrm{A}}\alpha_{im}(k)\,\mathrm{e}^{\mathrm{i}\boldsymbol{k}\cdot\boldsymbol{R}} \\
& \left. \times \sum_{\boldsymbol{\kappa},\,\epsilon} \left\{ \bar{e}_m^{(\epsilon)}(\boldsymbol{\kappa})\,e_n^{(\epsilon)}(\boldsymbol{\kappa}) \frac{\hbar c\kappa}{-\hbar ck-\hbar c\kappa}\,\mathrm{e}^{\mathrm{i}\boldsymbol{\kappa}\cdot\boldsymbol{R}} + e_m^{(\epsilon)}(\boldsymbol{\kappa})\,\bar{e}_n^{(\epsilon)}(\boldsymbol{\kappa}) \frac{\hbar c\kappa}{\hbar ck-\hbar c\kappa}\,\mathrm{e}^{-\mathrm{i}\boldsymbol{\kappa}\cdot\boldsymbol{R}} \right\} \right]. \quad (14)
\end{aligned}
$$

We digress at this point to note that it is possible to obtain the result (14) by using the effective two-photon interaction operator

$$
H_{\mathrm{eff\,int}}^{(\mathrm{A/B})} = -{}^{(\mathrm{A/B})}\alpha_{ij}(k)\,e_i^{\perp}(\boldsymbol{k}/\boldsymbol{k}')\,e_j^{\perp}(\boldsymbol{\kappa}) \quad (15)
$$

for the two chromophores. The use of (15) corresponds to 'collapsing' two one-photon vertices to a two-photon vertex in the time-ordered graphs. This may be achieved by a suitable canonical transformation of the multipolar Hamiltonian as in the study of induced circular dichroism (Craig, Power & Thirunamachandran 1976). An effective interaction Hamiltonian of the type (15) has also been used in the study of two-photon circular dichroism (Andrews 1976). The use of (15) allows the calculation to be carried out more simply using second-order perturbation theory with the aid of the four time-ordered diagrams shown in figure 4. Each of these diagrams represents the sum of a subset of twelve set $\{\alpha\}$ diagrams. For example, figure 4a represents the sum of the subset of graphs typified by figure 2a.

We now return to expression (14) and carry out the sum over the polarization and the wave vector of the virtual photon finding

$$
\begin{aligned}
M_{4\alpha}(\mathrm{L/R}) = & (8\pi^2\hbar ck/V)\,\bar{e}'_i e_j^{(\mathrm{L/R})}\,V_{mn}(k,\boldsymbol{R}) \\
& \times [{}^{\mathrm{A}}\alpha_{im}(k)\,{}^{\mathrm{B}}\alpha_{nj}(k)\,\mathrm{e}^{\mathrm{i}\boldsymbol{k}\cdot\boldsymbol{R}} + {}^{\mathrm{B}}\alpha_{im}(k)\,{}^{\mathrm{A}}\alpha_{nj}(k)\,\mathrm{e}^{-\mathrm{i}\boldsymbol{k}'\cdot\boldsymbol{R}}], \quad (16)
\end{aligned}
$$

where $V_{mn}(k,\boldsymbol{R})$ is the retarded dipole–dipole interaction tensor

$$
\begin{aligned}
V_{mn}(k,\boldsymbol{R}) = (1/4\pi R^3)\,[&(\delta_{mn}-3\hat{R}_m\hat{R}_n)\,(\cos kR + kR\sin kR) \\
& -(\delta_{mn}-\hat{R}_m\hat{R}_n)\,k^2R^2\cos kR]. \quad (17)
\end{aligned}
$$

In a similar manner we evaluate the set $\{\beta\}$ contributions to the matrix element and find

$$
\begin{aligned}
M_{4\beta}(\mathrm{L/R}) = & -(4\pi^2\hbar ck/V^2)\,\bar{e}'_i e_j^{(\mathrm{L/R})} \\
& \times [{}^{\mathrm{A}}\beta_{imj}(k)\,{}^{\mathrm{B}}\mu_n \sum_{\boldsymbol{\kappa},\,\epsilon}\{\bar{e}_m^{(\epsilon)}(\boldsymbol{\kappa})\,e_n^{(\epsilon)}(\boldsymbol{\kappa})\,\mathrm{e}^{\mathrm{i}\boldsymbol{\kappa}\cdot\boldsymbol{R}} + e_m^{(\epsilon)}(\boldsymbol{\kappa})\,\bar{e}_n^{(\epsilon)}(\boldsymbol{\kappa})\,\mathrm{e}^{-\mathrm{i}\boldsymbol{\kappa}\cdot\boldsymbol{R}}\} \\
& + {}^{\mathrm{B}}\beta_{imj}(k)\,{}^{\mathrm{A}}\mu_n\,\mathrm{e}^{\mathrm{i}(\boldsymbol{k}-\boldsymbol{k}')\cdot\boldsymbol{R}} \sum_{\boldsymbol{\kappa},\,\epsilon}\{e_m^{(\epsilon)}(\boldsymbol{\kappa})\,\bar{e}_n^{(\epsilon)}(\boldsymbol{\kappa})\,\mathrm{e}^{\mathrm{i}\boldsymbol{\kappa}\cdot\boldsymbol{R}} + \bar{e}_m^{(\epsilon)}(\boldsymbol{\kappa})\,e_n^{(\epsilon)}(\boldsymbol{\kappa})\,\mathrm{e}^{-\mathrm{i}\boldsymbol{\kappa}\cdot\boldsymbol{R}}\}], \quad (18)
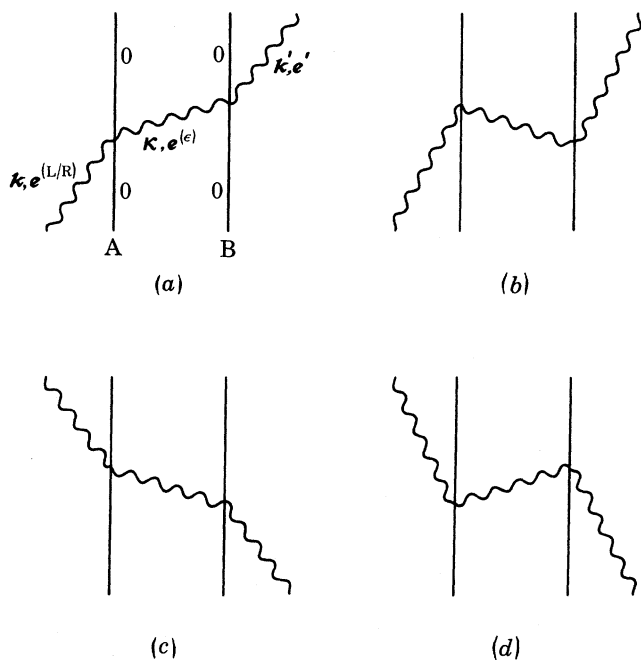\end{aligned}
$$

FIGURE 4. Time-ordered diagrams which use the effective interaction
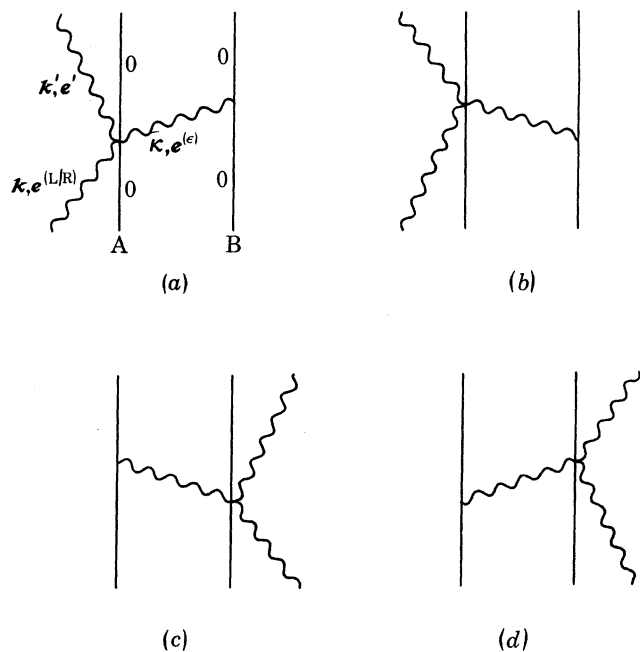Hamiltonian expression (15).

FIGURE 5. Time-ordered diagrams which use the effective interaction
Hamiltonian expression (20).

where $^A\mu$ and $^B\mu$ are the static dipole moments of A and B in their ground states. The tensor $^A\beta_{imj}(k)$ is given by

$$^A\beta_{imj}(k) = \sum_{r,s} \left\{ \frac{^A\mu_i^{0s}\,{}^A\mu_m^{sr}\,{}^A\mu_j^{r0}}{(E_{s0}^A - \hbar ck)(E_{r0}^A - \hbar ck)} + \frac{^A\mu_m^{0s}\,{}^A\mu_i^{sr}\,{}^A\mu_j^{r0}}{E_{s0}^A\,(E_{r0}^A - \hbar ck)} + \frac{^A\mu_m^{0s}\,{}^A\mu_j^{sr}\,{}^A\mu_i^{r0}}{E_{s0}^A\,(E_{r0}^A + \hbar ck)} \right.$$
$$\left. + \frac{^A\mu_i^{0s}\,{}^A\mu_j^{sr}\,{}^A\mu_m^{r0}}{(E_{s0}^A - \hbar ck)\,E_{r0}^A} + \frac{^A\mu_j^{0s}\,{}^A\mu_i^{sr}\,{}^A\mu_m^{r0}}{(E_{s0}^A + \hbar ck)\,E_{r0}^A} + \frac{^A\mu_j^{0s}\,{}^A\mu_m^{sr}\,{}^A\mu_i^{r0}}{(E_{s0}^A + \hbar ck)(E_{r0}^A + \hbar ck)} \right\} \quad (19)$$

and the summation is over the intermediate states $|r\rangle$ and $|s\rangle$ of A. A similar expression holds for $^B\beta_{imj}(k)$, and with the assumption of real wavefunctions it may be shown that these tensors are symmetric in the indices i and j. As with the diagrams of set $\{\alpha\}$, we can collapse the forty-eight diagrams of set $\{\beta\}$ into four diagrams (figure 5) with an effective three-photon interaction operator of the form

$$H_{\text{eff int}}^{(A/B)} = -{}^{(A/B)}\beta_{ijk}(k)\,e_i^\perp(k')\,e_j^\perp(\kappa)\,e_k^\perp(k) \quad (20)$$

for the chromophore scattering the real photon and the usual dipole interaction operator $-\mu \cdot e^\perp$ for the other. It is easily seen that the four terms in (18) correspond to the four graphs in figure 5. After performing the summations over the polarization and the wave vector of the virtual photon, the matrix element (18) becomes

$$M_{4\beta}(\text{L/R}) = \left(\frac{8\pi^2\hbar ck}{V}\right)\bar{e}_i'\,e_j^{(\text{L/R})}\,V_{mn}(0,R)\,[^A\beta_{imj}(k)\,^B\mu_n + {}^B\beta_{imj}(k)\,^A\mu_n\,\mathrm{e}^{\mathrm{i}(k-k')\cdot R}], \quad (21)$$

where $V_{mn}(0,R)$ is the dipole–dipole interaction tensor without retardation obtained from (17) by putting $k = 0$. Though the result is similar in form to the second-order result (11) we note that, unlike either the M_2 or the $M_{4\alpha}$ contributions, the result (21) vanishes if either chromophore has local inversion symmetry, for μ_n and $\beta_{imj}(k)$ are then both zero.

3. DIFFERENTIAL SCATTERING INTENSITIES

In this section we compute the difference in scattering intensities for incident right- and left-circularly polarized photons. The differential scattering evidently depends on the polarization of the emergent radiation. Most observations are made for the case where e', the polarization vector of the scattered photon, is either in the $\hat{k}\hat{k}'$-plane or normal to it. We denote the former by $e^{\parallel}$ and the latter by $e^\perp$. The three unit vectors $e^{\parallel}$, $e^\perp$ and $\hat{k}'$ form a right handed set.

We first write down the scattering rate using the Fermi rule:

$$\Gamma = (2\pi/\hbar)\,|M_2 + M_{4\alpha} + M_{4\beta} + \ldots|^2 \rho_f \quad (22)$$

$$\approx (2\pi/\hbar)\,[\,|M_2|^2 + M_2\bar{M}_{4\alpha} + \bar{M}_2 M_{4\alpha} + M_2\bar{M}_{4\beta} + \bar{M}_2 M_{4\beta}]\,\rho_f. \quad (23)$$

In equations (22) and (23) we have suppressed the polarization indices of both the incident and scattered photons. In (23) the first term within the brackets is the second-order contribution arising from the uncoupled graphs (figure 1). The

remaining terms represent the interference between the second-order and fourth-order amplitudes. Higher-order contributions are small and can be neglected. Noting that the scattered radiant intensity I' (power per unit solid angle about $\hat{k}'$) is equal to the irradiance I_0 (power per unit area) of the incident beam times the scattering cross section, we have

$$I' = I_0 \left(\frac{kV}{2\pi\hbar c}\right)^2 |M|^2. \tag{24}$$

M_2–M_2 *contributions.* It is convenient to consider separately the contributions to the scattered intensities resulting from the interference of the second-order amplitudes and the contributions from the second- and fourth-order amplitudes. The differential intensity correct to second order is

$$I'(\mathrm{R}) - I'(\mathrm{L}) \equiv \Delta I' = I_0 \left(\frac{kV}{2\pi\hbar c}\right)^2 [|M_2(\mathrm{R})|^2 - |M_2(\mathrm{L})|^2]. \tag{25}$$

Inserting (11) in (25) we get

$$\Delta I' = I_0 k^4 e_i' e_k' (e_j^{(\mathrm{R})} e_l^{(\mathrm{L})} - e_j^{(\mathrm{L})} e_l^{(\mathrm{R})}) [^{\mathrm{A}}\alpha_{ij}{}^{\mathrm{A}}\alpha_{kl} + {}^{\mathrm{B}}\alpha_{ij}{}^{\mathrm{B}}\alpha_{kl}$$
$$+ {}^{\mathrm{A}}\alpha_{ij}{}^{\mathrm{B}}\alpha_{kl} e^{-\mathrm{i}(k-k')\cdot R} + {}^{\mathrm{B}}\alpha_{ij}{}^{\mathrm{A}}\alpha_{kl} e^{\mathrm{i}(k-k')\cdot R}], \tag{26}$$

where α is assumed to be real and its k-dependence is implicit; also $\bar{e}' = e'$ for the linearly polarized photon. Since $^{\mathrm{A}}\alpha_{ij}{}^{\mathrm{A}}\alpha_{kl}$ and $^{\mathrm{B}}\alpha_{ij}{}^{\mathrm{B}}\alpha_{kl}$ are symmetric to interchange of i and k together with the interchange of j and l, and the polarization factor $e_i' e_k'(e_j^{(\mathrm{R})} e_l^{(\mathrm{L})} - e_j^{(\mathrm{L})} e_l^{(\mathrm{R})})$ is antisymmetric, the first two terms in (26) do not contribute and we get

$$\Delta I' = I_0 k^4 e_i' e_k' (\mathrm{i}\epsilon_{jlm}\hat{k}_m) [^{\mathrm{A}}\alpha_{ij}{}^{\mathrm{B}}\alpha_{kl} e^{-\mathrm{i}(k-k')\cdot R} + {}^{\mathrm{B}}\alpha_{ij}{}^{\mathrm{A}}\alpha_{kl} e^{\mathrm{i}(k-k')\cdot R}], \tag{27}$$

where we have used the identity

$$e_j^{(\mathrm{R})}(\boldsymbol{k}) e_l^{(\mathrm{L})}(\boldsymbol{k}) - e_j^{(\mathrm{L})}(\boldsymbol{k}) e_l^{(\mathrm{R})}(\boldsymbol{k}) = \mathrm{i}\epsilon_{jlm}\hat{k}_m. \tag{28}$$

One feature of the conventional experiments is that because the observations are made in fluid phase the molecules are randomly oriented with respect to the incident radiation. In order to relate the calculated result to experiment, it is necessary to perform a rotational average on (27). For this purpose we need to refer the components of R and the scattering tensors to a molecule-fixed frame. Using the Euler angle matrix to relate this frame to the laboratory frame, we can carry out the rotational average of (27) for the two cases, namely when $e' = e^{\parallel}$ or $e^{\perp}$, and we obtain

$$\Delta I_{2,2}^{\parallel} = -2\sqrt{2}\, I_0 k^4 (1-\cos\theta)^{\frac{3}{2}} \epsilon_{\nu\pi\tau} \hat{R}_{\tau}{}^{\mathrm{A}}\alpha_{\lambda\nu}{}^{\mathrm{B}}\alpha_{\mu\pi} [(\delta_{\lambda\mu} - \hat{R}_{\lambda}\hat{R}_{\mu})\mathscr{I}_1(a) + \hat{R}_{\lambda}\hat{R}_{\mu}\mathscr{I}_2(a)] \tag{29}$$

and

$$\Delta I_{2,2}^{\perp} = -4\sqrt{2}\, I_0 k^4 (1-\cos\theta)^{\frac{1}{2}} \epsilon_{\nu\pi\tau} \hat{R}_{\tau}{}^{\mathrm{A}}\alpha_{\lambda\nu}{}^{\mathrm{B}}\alpha_{\mu\pi} [(\delta_{\lambda\mu} - \hat{R}_{\lambda}\hat{R}_{\mu})\mathscr{I}_1(a) + \hat{R}_{\lambda}\hat{R}_{\mu}\mathscr{I}_2(a)]. \tag{30}$$

In equations (29) and (30), $\cos\theta = \hat{\boldsymbol{k}}.\hat{\boldsymbol{k}}'$; Greek indices denote components relative to the molecular frame. The functions $\mathscr{I}_1$ and $\mathscr{I}_2$ arise from the Euler angle averages and are given by†

$$\mathscr{I}_1(x) = \frac{1}{8}\left[\frac{\cos x}{x} - 2\frac{\sin x}{x^2} - 3\frac{\cos x}{x^3} + 3\frac{\sin x}{x^4}\right], \tag{31}$$

$$\mathscr{I}_2(x) = \frac{1}{2}\left[\frac{\sin x}{x^2} + 3\frac{\cos x}{x^3} - 3\frac{\sin x}{x^4}\right] \tag{32}$$

and

$$a = |\boldsymbol{k} - \boldsymbol{k}'|\,R = \sqrt{2}\,kR(1 - \cos\theta)^{\frac{1}{2}}. \tag{33}$$

It is important to note that $\mathscr{I}_1(a)$ and $\mathscr{I}_2(a)$ in (29) and (30) depend on the scattering angle. Also the ratio of the two differential intensities depends on the scattering angle alone, according to the relation

$$\Delta I_{2,2}^{\perp} = 2(1 - \cos\theta)^{-1}\Delta I_{2,2}^{\parallel}. \tag{34}$$

A detailed discussion of these results including their asymptotic behaviour is reserved for a later section.

M_2–$M_{4\alpha}$ *contributions.* Using the matrix elements (11) and (16), we find the contribution to the scattered intensity for fixed molecular orientation:

$$I_{2,4\alpha}'(\mathrm{L/R}) = I_0\left(\frac{kV}{2\pi\hbar c}\right)^2 [M_2(\mathrm{L/R})\bar{M}_{4\alpha}(\mathrm{L/R}) + \mathrm{c.c.}] \tag{35}$$

$$= -4\pi I_0 k^4 V_{mn}(k,\boldsymbol{R})\,e_i' e_j^{(\mathrm{L/R})} e_k' \bar{e}_l^{(\mathrm{L/R})}$$
$$\times [{}^A\alpha_{ij}{}^B\alpha_{km}{}^A\alpha_{nl}\,\mathrm{e}^{\mathrm{i}\boldsymbol{k}'\cdot\boldsymbol{R}} + {}^B\alpha_{ij}{}^A\alpha_{km}{}^B\alpha_{nl}\,\mathrm{e}^{-\mathrm{i}\boldsymbol{k}'\cdot\boldsymbol{R}}$$
$$+ {}^A\alpha_{ij}{}^B\alpha_{nl}{}^A\alpha_{km}\mathrm{e}^{-\mathrm{i}\boldsymbol{k}\cdot\boldsymbol{R}} + {}^B\alpha_{ij}{}^A\alpha_{nl}{}^B\alpha_{km}\mathrm{e}^{\mathrm{i}\boldsymbol{k}\cdot\boldsymbol{R}}] + \mathrm{c.c.}, \tag{36}$$

where c.c. stands for complex conjugate. It is now a straightforward matter to compute the differential intensities for random molecular orientation; we give below the results for the two polarizations of the scattered photon,

$$\Delta I_{2,4\alpha}^{\parallel} = -8\pi I_0 k^4 V_{\rho\sigma}(k,\boldsymbol{R})\,\epsilon_{\nu\tau\tau}\hat{R}_\tau[4(\mathscr{I}_1(b) - \mathscr{I}_2(b))$$
$$\times \{\cos\theta(\delta_{\lambda\mu} - \hat{R}_\lambda\hat{R}_\mu)({}^A\alpha_{\lambda\nu}{}^B\alpha_{\mu\rho}{}^A\alpha_{\sigma\pi} - \cos\theta\,{}^A\alpha_{\lambda\nu}{}^B\alpha_{\pi\rho}{}^A\alpha_{\sigma\mu})$$
$$+ 2(\cos^2\theta - 1)\hat{R}_\lambda\hat{R}_\mu{}^A\alpha_{\lambda\nu}{}^B\alpha_{\pi\rho}{}^A\alpha_{\sigma\mu}\}$$
$$+ \mathscr{I}_2(b)\{(3\cos^2\theta + \cos\theta - 2)\,{}^A\alpha_{\lambda\lambda}{}^B\alpha_{\nu\rho}{}^A\alpha_{\sigma\pi}$$
$$- (3\cos^2\theta - 3\cos\theta - 2)\,{}^A\alpha_{\lambda\nu}{}^B\alpha_{\lambda\rho}{}^A\alpha_{\sigma\pi}$$
$$+ (\cos^2\theta + \cos\theta - 4)\,{}^A\alpha_{\lambda\nu}{}^B\alpha_{\pi\rho}{}^A\alpha_{\sigma\lambda}\}$$
$$\text{— terms obtained by interchanging A and B],} \tag{37}$$

$$\Delta I_{2,4\alpha}^{\perp} = -8\pi I_0 k^4 V_{\rho\sigma}(k,\boldsymbol{R})\,\epsilon_{\nu\pi\tau}\hat{R}_\tau[4(\mathscr{I}_1(b) - \mathscr{I}_2(b))$$
$$\times (\delta_{\lambda\mu} - \hat{R}_\lambda\hat{R}_\mu)(\cos\theta\,{}^A\alpha_{\lambda\nu}{}^B\alpha_{\mu\rho}{}^A\alpha_{\sigma\pi} - {}^A\alpha_{\lambda\nu}{}^B\alpha_{\pi\rho}{}^A\alpha_{\sigma\mu})$$
$$+ \mathscr{I}_2(b)\{(\cos\theta + 1)\,{}^A\alpha_{\lambda\lambda}{}^B\alpha_{\nu\rho}{}^A\alpha_{\sigma\pi} + (3\cos\theta - 1)\,{}^A\alpha_{\lambda\nu}{}^B\alpha_{\lambda\rho}{}^A\alpha_{\sigma\pi}$$
$$+ (\cos\theta - 3)\,{}^A\alpha_{\lambda\nu}{}^B\alpha_{\pi\rho}{}^A\alpha_{\sigma\lambda}\}$$
$$\text{— terms obtained by interchanging A and B].} \tag{38}$$

† The functions $\mathscr{I}_1$ and $\mathscr{I}_2$ as defined by (31) and (32) differ by a factor i from those previously used by Andrews (1976).

In writing (37) and (38) we have used the fact that $V_{\rho\sigma}$ is real and symmetric in ρ, σ, and $b = kR$. Here no simple relation exists between the results for the two polarizations.

M_2–$M_{4\beta}$ *contributions.* We recall that the relevant fourth-order graphs are those where absorption and emission of the real photons occur at the same centre. Also, the coupling potential in the matrix element is non-retarded. This leads to a similarity in the forms of M_2 and $M_{4\beta}$ terms in (11) and (21) respectively. Consequently, the M_2–$M_{4\beta}$ interference contribution to the scattered intensity can be calculated in a manner analogous to the second-order terms. Suppppressing the details of the calculation, we give the randomly averaged results for $e' = e^{\|}$ and $e^{\perp}$:

$$\Delta I_{2,4\beta}^{\|} = 8\sqrt{2}\,\pi I_0 k^4 (1 - \cos\theta)^{\frac{3}{2}} V_{\rho\sigma}(0, \mathbf{R})\,\epsilon_{\nu\pi\tau}\hat{R}_\tau$$

$$\times [(\delta_{\lambda\mu} - \hat{R}_\lambda \hat{R}_\mu)\,\mathscr{I}_1(a) + \hat{R}_\lambda \hat{R}_\mu \mathscr{I}_2(a)]\,[^{A}\alpha_{\lambda\nu}\,^{B}\beta_{\mu\rho\pi}\,^{A}\mu_\sigma - ^{B}\alpha_{\lambda\nu}\,^{A}\beta_{\mu\rho\pi}\,^{B}\mu_\sigma] \quad (39)$$

and
$$\Delta I_{2,4\beta}^{\perp} = 2(1 - \cos\theta)^{-1}\,\Delta I_{2,4\beta}^{\|} \quad (40)$$

with $a = |\mathbf{k} - \mathbf{k}'|R$. The expressions (39) and (40) vanish for centrosymmetric chromophores.

The full expressions for the differential intensities correct to order indicated by terms M_2–M_4 are obtained by summing (29), (37) and (39) for the 'in-plane' component of the scattered radiation, and (30), (38) and (40) for the perpendicular component. These expressions are linearly dependent on the intensity of the incident radiation. However, it is possible to present them in a form which is independent of the intensity. For this purpose, we define the differential ratio

$$\Delta^{(\lambda)} = \frac{I^{(\lambda)}(\mathrm{R}) - I^{(\lambda)}(\mathrm{L})}{I^{(\lambda)}(\mathrm{R}) + I^{(\lambda)}(\mathrm{L})}. \quad (41)$$

From (23) we note that the dominant contribution to the absolute scattered intensity comes from the square of the second-order term; thus

$$I^{(\lambda)}(\mathrm{R}) + I^{(\lambda)}(\mathrm{L}) \approx I_0 k^4 e_i' e_k' (e_j^{(\mathrm{R})} e_l^{(\mathrm{L})} + e_j^{(\mathrm{L})} e_l^{(\mathrm{R})})$$

$$\times [^{A}\alpha_{ij}\,^{A}\alpha_{kl} + ^{B}\alpha_{ij}\,^{B}\alpha_{kl} + ^{A}\alpha_{ij}\,^{B}\alpha_{kl}\,\mathrm{e}^{-\mathrm{i}(k-k')\cdot\mathbf{R}} + ^{B}\alpha_{ij}\,^{A}\alpha_{kl}\,\mathrm{e}^{\mathrm{i}(k-k')\cdot\mathbf{R}}]. \quad (42)$$

Using the relation
$$e_j^{(\mathrm{R})}(\mathbf{k})\,e_l^{(\mathrm{L})}(\mathbf{k}) + e_j^{(\mathrm{L})}(\mathbf{k})\,e_l^{(\mathrm{R})}(\mathbf{k}) = (\delta_{jl} - \hat{k}_j \hat{k}_l) \quad (43)$$

in (42) and performing the rotational average, we obtain for the two different polarizations

$$I^{\|}(\mathrm{R}) + I^{\|}(\mathrm{L}) \approx \left(\frac{I_0 k^4}{30}\right)[(3\cos^2\theta - 2)\,(^{A}\alpha_{\lambda\lambda} + ^{B}\alpha_{\lambda\lambda})^2$$

$$+ (\cos^2\theta + 6)\,(^{A}\alpha_{\lambda\mu}\,^{A}\alpha_{\lambda\mu} + ^{B}\alpha_{\lambda\mu}\,^{B}\alpha_{\lambda\mu} + 2\,^{A}\alpha_{\lambda\mu}\,^{B}\alpha_{\lambda\mu})] \quad (44)$$

and

$$I^{\perp}(\mathrm{R}) + I^{\perp}(\mathrm{L}) \approx \left(\frac{I_0 k^4}{30}\right)[(^{A}\alpha_{\lambda\lambda} + ^{B}\alpha_{\lambda\lambda})^2 + 7(^{A}\alpha_{\lambda\mu}\,^{A}\alpha_{\lambda\mu} + ^{B}\alpha_{\lambda\mu}\,^{B}\alpha_{\lambda\mu} + 2\,^{A}\alpha_{\lambda\mu}\,^{B}\alpha_{\lambda\mu})]. \quad (45)$$

These expressions together with the total differential scattering intensities lead to the evaluation of the circular intensity differential ratio (41).

4. DISCUSSION

The results in the previous section are based on a calculation complete to the fourth order with the assumption that the chromophores are inherently optically inactive, i.e. do not, in isolation, cause differential scattering. Also, compatibly with the electric dipole approximation (7), their *individual* sizes must be small compared with the reduced wavelength $\lambdabar$ ($= 1/k$) of the incident radiation. There is no restriction on the magnitude of the inter-chromophore separation and a complete account of retardation is included. It is instructive to examine the expressions for the differential scattering intensities for the two limiting cases: (a) R small compared with $\lambdabar$, i.e. $kR \ll 1$; (b) R large compared with $\lambdabar$, i.e. $kR \gg 1$. In the region (a), although R is small compared with $\lambdabar$, it must be sufficiently large to make the retardation effects significant. The limiting case (a) is physically realizable for many molecules. Case (b) is important in the study of differential scattering by macromolecules. For systems where neither limit is applicable, it is essential to use the complete expressions for the calculation of differential intensities.

Case (a) $R \ll \lambdabar$. An examination of the differential intensity expressions (29) and (30), which are correct to second order, shows that the asymptotic behaviour depends on the R-dependent coefficients $\mathscr{I}_1$ and $\mathscr{I}_2$. It is easily seen that for small values of a, the leading terms of $\mathscr{I}_1$ and $\mathscr{I}_2$ are equal,

$$\mathscr{I}_1(a) = \mathscr{I}_2(a) \simeq -\tfrac{1}{30}a \quad (a \ll 1), \tag{46}$$

where we recall that $a = |\mathbf{k} - \mathbf{k}'| R = \sqrt{2}\, kR(1 - \cos\theta)^{\frac{1}{2}}$. Using (46) we find that the differential intensity expressions become

$$\Delta I_{2,2}^{\parallel} \simeq (\tfrac{2}{15}) I_0 k^5 R(1 - \cos\theta)^2 \epsilon_{\nu\pi\tau} \hat{R}_\tau {}^{A}\alpha_{\lambda\nu} {}^{B}\alpha_{\lambda\pi}, \tag{47}$$

$$\Delta I_{2,2}^{\perp} \simeq 2(1 - \cos\theta)^{-1} \Delta I_{2,2}^{\parallel}. \tag{48}$$

We note that the differential effect depends on $\sin^4(\tfrac{1}{2}\theta)$ for the parallel polarization component and $\sin^2(\tfrac{1}{2}\theta)$ for the perpendicular component. These functions clearly reach maximum values for backward scattering when the two differential intensity components become equal.

The above results, (47) and (48), may also be obtained from (27) by first expanding the exponentials and then retaining the leading term after rotational averaging. We remark in passing that it is also possible to obtain these results for the region $R \ll \lambdabar$ by noting the origin dependence of multiple moments (Barron & Buckingham 1974). An important property of these limiting expressions is their linear dependence on R in the near-zone.

The analysis of the second-order–fourth-order interference terms in this region follows similar lines except for the modification resulting from the R-dependent interaction tensor $V_{\rho\sigma}(k, \mathbf{R})$ in (37) and (38) and $V_{\rho\sigma}(0, \mathbf{R})$ in (39) and (40). For small kR,

$$V_{\rho\sigma}(k, \mathbf{R}) \simeq V_{\rho\sigma}(0, \mathbf{R}) = (1/4\pi R^3)(\delta_{\rho\sigma} - 3\hat{R}_\rho \hat{R}_\sigma) \quad (kR \ll 1). \tag{49}$$

Consequently, these differential intensity terms vary as R^{-2}. A comparison of the different terms contributing to the differential intensities shows that the two types

of second-order–fourth-order interference terms are comparable in magnitude, and are smaller than the second-order term by a factor of the same magnitude as the polarizability of the chromophore divided by R^3.

Case (b) $R \gg \lambda$. In this region, the coefficient $\mathscr{I}_1(x)$, equation (31), tends to $(\cos x)/8x$ when $x = kR$. Also, when the scattering is not near the forward direction $\mathscr{I}_1(x)$ exhibits the same asymptotic behaviour for $x = |\boldsymbol{k} - \boldsymbol{k'}| R$. The leading term of $\mathscr{I}_2$ is of higher inverse power dependence on x and may be ignored. Consequently, the second-order terms (29) and (30) fall off with a modulated R^{-1} dependence in this region, whereas in the near-zone they vary linearly with R. The two types of interference terms behave differently in the far-zone because of the difference in the asymptotic behaviour of $V_{\rho\sigma}(k, \boldsymbol{R})$ and $V_{\rho\sigma}(0, \boldsymbol{R})$. From (17) we note that

$$V_{\rho\sigma}(k, \boldsymbol{R}) \simeq -(k^2/4\pi R)(\delta_{\rho\sigma} - \hat{R}_\rho \hat{R}_\sigma) \cos kR \quad (kR \gg 1). \tag{50}$$

Apart from modulating factors, the expressions (37) and (38) for $\Delta I'_{2,4\alpha}$ vary as R^{-2} in this region, whereas those for $\Delta I'_{2,4\beta}$, (39) and (40), fall off as R^{-4}; the latter may therefore be ignored.

No experimental data on differential Rayleigh scattering are available as yet. When experimental techniques are developed, the use of a suitable series of chemically similar compounds should enable the dependence of the differential intensities on the scattering angle and the group separation to be confirmed.

REFERENCES

Andrews, D. L. 1976 *Chem. Phys.* **16**, 419.
Andrews, D. L. & Thirunamachandran, T. 1978 *Proc. R. Soc. Lond.* A **358**, 311.
Babiker, M., Power, E. A. & Thirunamachandran, T. 1974 *Proc. R. Soc. Lond.* A **338**, 235.
Barron, L. D., Bogaard, M. P. & Buckingham, A. D. 1973 *J. Am. chem. Soc.* **95**, 603.
Barron, L. D. & Buckingham, A. D. 1971 *Molec. Phys.* **20**, 1111.
Barron, L. D. & Buckingham, A. D. 1974 *J. Am. chem. Soc.* **96**, 4769.
Bhagavantam, S. & Venkateswaran, S. 1930 *Nature, Lond.* **125**, 237.
Craig, D. P., Power, E. A. & Thirunamachandran, T. 1976 *Proc. R. Soc. Lond.* A **348**, 19.
Kastler, A. 1930 *C. r. hebd. Séanc. Acad. Sci., Paris* **191**, 565.
Kirkwood, J. G. 1937 *J. chem. Phys.* **5**, 479.
Stone, A. J. 1977 *Molec. Phys.* **33**, 293.